Trumpet sound simulation using a two-dimensional lip vibration model

Seiji Adachi[a] and Masa-aki Sato
ATR Human Information Processing Research Laboratories, 2-2, Hikaridai, Seika-cho, Soraku-gun, Kyoto, 619-02 Japan

(Received 6 January 1995; revised 26 September 1995; accepted 17 October 1995)

Trumpet sound simulation is carried out with a two-dimensional lip vibration model, where the lips execute both swinging and stretching motions. This model allows lips to operate on both the lower and higher frequency sides of the air-column resonance frequencies. Oscillations generated by the total sound production system are on both the lower and higher frequency sides in the first through third resonance modes, while in the fourth and higher modes they are realized only on the lower side. From each resonance mode, an oscillation having the least frequency deviation against a change in lip eigenfrequency and also having sufficient amplitude is selected as the optimum oscillation of the resonance mode. It is found that these oscillations in the lower modes have positive phase differences between lip vibration and mouthpiece pressure, whereas those in the higher modes have negative ones. This result closely matches the transition of lip vibration states from the one modeled by the outward-striking valve at the second mode (i.e., the lowest mode among those used musically) to that modeled by the laterally striking valve at the higher modes, which is observed in the simultaneous measurement of mouthpiece pressure and lip vibration.

PACS numbers: 43.75.Fg

INTRODUCTION

According to Helmholtz,[1] reeds of woodwind instruments such as clarinets, oboes, and bassoons are classified as having a valve that strikes inward [Fig. 1(a)] and tend to close in increments of blowing pressure, whereas lip reeds of brass instruments like trumpets, trombones, and French horns are classified as having a valve that strikes outward [Fig. 1(b)] and open further in the same condition. This classification has been widely accepted, and there is no doubt that woodwind reeds should be classified as striking inward.

There are, however, arguments against the classification of the lip reeds. Unlike the mechanical cane reeds of woodwind instruments that have definite constraints on their directions of motion, biological lips deform quite unrestrictively when they are used as a lip-reed generator put to the mouthpiece. Moreover, a player's embouchure drastically varies the constraints on lips for the frequency, sound level and spectrum of sound. Furthermore, stroboscopic measurements by Martin,[2] Leno,[3] and Copley and Strong[4] of the brass instrument player's lips reveal that their two-dimensional motion is both parallel and perpendicular to the direction of flow. Therefore, careful consideration of lip vibration is needed, and other possibilities of modeling should be examined.

Elliott and Bowsher[5] raise the possibility that the lips are, in part, driven laterally—perpendicular to the direction of flow—by the time-varying Bernoulli pressure at the lip opening by analogy to vocal-fold vibration, although their main concern is to investigate the outward-striking lip-reed model. Saneyoshi *et al.*[6] investigated a ''transverse'' model[7] [Fig. 1(c)] in which the Bernoulli pressure drives a retracting valve (representing the upper lip) at a right angle to the direction of flow; their model successfully explains the mechanism of mode selection in a euphonium. Fletcher presented a unified discussion of the general conditions under which oscillation of these three types of valve configurations occurs.[8]

Models of lip vibration influence phase relations among the variables that describe the self-oscillation of the brass instrument: mouthpiece pressure p, air volume velocity flowing into the mouthpiece, U, and the area of the lip opening, S_{lip}. In the ''outward-striking'' model, S_{lip} and p are out of phase in the low-frequency region, where frequency f is sufficiently smaller than the lip eigenfrequency f_{lip}. This is because the valve, representing the lip, is drawn into the instrument and thus opens as p decreases. On the other hand, in the transverse model, S_{lip} and p are in phase in this frequency region because the Bernoulli pressure generated by the flow at the lip opening tends to close the valve as p decreases. In the frequency region near f_{lip}, where the lips are actually driven, the phase shift due to the lip resonance occurs in both models. Therefore, the phase difference $\angle S_{\mathrm{lip}} - \angle p$ becomes about 90° in the outward-striking model and $-90°$ in the transverse model.

Suppose that the linear theory[5,9] of self-oscillation is valid, U is proportional to S_{lip} regardless of frequency, and thus they oscillate in phase. This immediately requires the phase of the input impedance Z_{in}, which is defined by the ratio p/U, to be about $-90°$ in the outward-striking model and 90° in the transverse model. Due to the resonance characteristics of the instrument, $\angle Z_{\mathrm{in}}$ varies rapidly from a positive value around 90° to a negative value around $-90°$ as frequency f rises and sweeps each resonance frequency (i.e., frequency of each input impedance peak). It is therefore ex-

[a]E-mail: adachi@hip.atr.co.jp

 0001-4966/96/99(2)/1200/10/$6.00

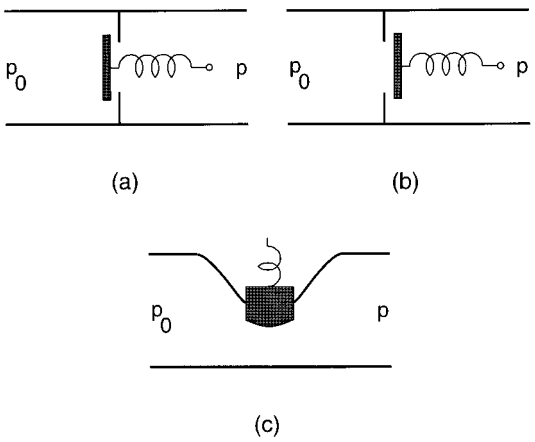

FIG. 1. Three different configurations of a pressure-controlled valve in an acoustic tube. In each configuration, p_0 is pressure in the upstream region of the valve, i.e., blowing pressure, and p is pressure in the downstream region of the valve, i.e., mouthpiece pressure. (a) Inwardly striking valve, which tends to close in increments of blowing pressure p_0. (b) Outwardly striking valve, which opens further as p_0 increases. (c) Retracting valve that strikes laterally to the direction of the flow. The Bernoulli pressure generated by the airflow tends to close this valve. Panel (a) models reeds of the woodwind instruments. (b) and (c) provide brass instrument lip-reed models in the lower and higher modes, respectively.

pected that the outward-striking model operates on the higher frequency side of the input impedance peaks, and the transverse model operates on the lower side.

In actual sound production, where the amplitude of oscillation is not always small enough for the linear theory to be applied, it is necessary to consider the nonlinearity of the system with a method such as time-domain simulation. Adachi and Sato[10] carried out a time-domain simulation of the brass instrument with two different one-dimensional lip vibration models, the ''swinging-door'' model and the transverse model. The former model employs a valve operating as a swinging door opening toward the downstream of the airflow and is essentially equivalent to the outward-striking model. Oscillation can be generated at the various resonance modes with both models. In their simulation systems, as the linear theory predicts, oscillation is always obtained on the higher frequency side with the swinging-door model and on the lower side with the transverse model.

Recent developments in lip modeling have been concerned with the two-dimensional behavior of lip motion. Keefe proposed a lip model that allows a single mass to oscillate in both the parallel and perpendicular directions.[11] He carried out a frequency domain analysis to show that oscillations can be sustained with both positive and negative phase differences between S_{lip} and p. This was controlled by a parameter representing the angle of lip inclination, which should depend upon the mouthpiece geometry and the player's embouchure.

Strong and Dudley[12] modeled lip motion in another way: They employed a swinging–sliding door having one degree of rotational freedom and one degree of translational freedom. They carried out a time-domain simulation of oscillations in the second resonance mode. Their simulation presents realistic mouthpiece pressure waveforms and reasonable spectrum variations according to the sound level. Although they did not show the phase relations, their obtained sounding frequencies imply that oscillations occur on both the higher and lower sides of the resonance frequency.

Yoshikawa[13] succeeded in measuring the phase difference between lip vibration and mouthpiece pressure while various acoustic tubes, including the French horn and the trumpet, are blown. His results with these instruments are summarized as follows: (1) Both instruments exhibit a positive phase difference in the second resonance mode (i.e., the lowest among those used musically); (2) in the higher modes (third and higher for the french horn, fourth for the trumpet), the phase difference is negative; and (3) oscillation in the third mode of the trumpet is possible with both positive and negative phase differences. These results indicate that lip vibration is better understood by the outward-striking model in the lower resonance modes and by the transverse model in the higher modes. At the same time, however, they imply that it is impossible to explain the change in phase relation with either one-dimensional model.

This paper presents a two-dimensional lip vibration model that can replicate the change in phase relation. This model is a combination of the two one-dimensional models, the swinging-door model and the transverse model. The modeled lip executes not only the swinging motion as a hinged door but also the stretching and contracting motion along the lip length. No deformation along the lip thickness is assumed. As in the case of the swinging-door model, the swinging motion corresponds to the outward-striking motion. On the other hand, the stretching and contracting motion corresponds to the laterally striking motion, because it is excited by the Bernoulli pressure at the lip opening in the same way as a retracting valve in the transverse model is driven.

This two-dimensional model has the capability to operate on either frequency side of the input impedance peaks, depending on which of the swinging and stretching motions is dominant. If the swinging motion becomes dominant, the oscillation has a positive phase difference between S_{lip} and p, and a frequency greater than one of the resonance frequencies. However, if the stretching motion becomes dominant, the oscillation with the negative phase difference, $\angle S_{\mathrm{lip}} - \angle p < 0$, is generated on the lower frequency side of the input impedance peaks. The main concern in this paper is to determine the actual behavior of the two-dimensional lip when it is incorporated into a total sound production system; making this determination with certainty requires the use of a time-domain simulation.

Section I is devoted to modeling the two-dimensional lip and incorporating it into a total sound production system. In Sec. II, the simulation method is first explained, and then the mode selection and oscillating quantities obtained in the simulation are examined. Section III discusses the mechanism of change between the lip vibration states in detail. Finally, the results of the simulation are summarized in Sec. IV.

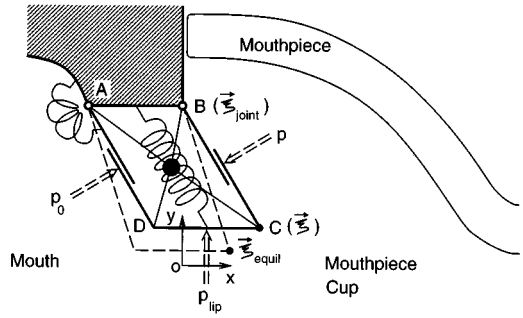

FIG. 2. Two-dimensional lip vibration model. The upper and lower lips are assumed to have symmetric motion. The modeled lip represented by the parallelogram ABCD simultaneously executes both swinging motion with the free joint AB and stretching motion along the sides BC and AD. The two springs supply restoring force for swinging and stretching displacements. The swinging motion is mainly driven by the pressure difference between the player's mouth and the mouthpiece, p_0-p, whereas the stretching motion is driven by the Bernoulli pressure p_{lip}.

I. MODEL

A. Two-dimensional lip vibration model

For simplicity, the upper and lower lips are assumed to have symmetric motion about the axis of the airflow. The dynamics of only the upper lip are thus considered. The lip is approximated as a simple mechanical oscillator composed of one mass, stiffness, and damping. Figure 2 depicts the schematic diagram of the two-dimensional lip model. The body of the lip is represented by a parallelogram ABCD. The upper side, AB, functions as a free joint connecting the lip with its base (hatched area). The BC and AD sides can vary their length l, while the AB and DC sides are assumed to be rigid and have a constant length d. Therefore, the lip simultaneously executes both swinging and stretching motions. Or equivalently, the tip of the lip, C, moves in directions both parallel (x axis) and perpendicular (y axis) to the airflow. The position of C is assigned by a two-dimensional vector $\boldsymbol{\xi}$. Likewise, the position of B is assigned by a constant vector $\boldsymbol{\xi}_{\mathrm{joint}}$. We call l and d the lip length and thickness, respectively. In the vector notation, the lip length is represented by $l=|\boldsymbol{\xi}-\boldsymbol{\xi}_{\mathrm{joint}}|$.

Lip mass m is assumed to be localized at the center of the lip. This implies that the moment of inertia with respect to the rotation about the center of the lip is omitted.

Two springs attached to the lip supply the restoring force: One is for swinging motion and the other is for stretching motion. When the lip is at rest, C is at a position indicated by $\boldsymbol{\xi}_{\mathrm{equil}}$. If the tip displaces from the rest position, force $\mathbf{F}_{\mathrm{restore}}$ having the direction pointing to $\boldsymbol{\xi}_{\mathrm{equil}}$ and the magnitude proportional to $|\boldsymbol{\xi}-\boldsymbol{\xi}_{\mathrm{equil}}|$ is supplied. This is another description of the lip having two springs with the same stiffness along the x- and y directions.

There are two different external forces driving the lip. One is the force $\mathbf{F}_{\Delta p}$ acting on the BC and AD sides, which is generated by the difference between the blowing pressure p_0 and the mouthpiece pressure p. Another external force is $\mathbf{F}_{\mathrm{Bernoulli}}$ acting on the DC side, which is generated by the Bernoulli pressure or the pressure at the lip opening p_{lip}.

The equation of lip motion is given by

$$\frac{1}{2}\,m\,\frac{d^2\boldsymbol{\xi}}{dt^2}=-\frac{1}{2}\,\frac{\sqrt{mk}}{Q}\,\frac{d\boldsymbol{\xi}}{dt}+\mathbf{F}_{\mathrm{restore}}+\mathbf{F}_{\Delta p}+\mathbf{F}_{\mathrm{Bernoulli}}, \quad (1)$$

with stiffness factor k and quality factor Q. The first terms in the left- and right-hand sides of Eq. (1) represent the inertia and the damping force, respectively. The factor of $\frac{1}{2}$ in these terms implies that the acceleration and velocity of the lip center are half as much as those of the tip $\boldsymbol{\xi}$. The forces $\mathbf{F}_{\mathrm{restore}}$, $\mathbf{F}_{\Delta p}$, and $\mathbf{F}_{\mathrm{Bernoulli}}$ can be written as follows:

$$\mathbf{F}_{\mathrm{restore}}=-\tfrac{1}{2}k(\boldsymbol{\xi}-\boldsymbol{\xi}_{\mathrm{equil}}), \quad (2)$$

$$\mathbf{F}_{\Delta p}=b(p_0-p)(\boldsymbol{\xi}-\boldsymbol{\xi}_{\mathrm{joint}})^{\perp}, \quad (3)$$

$$\mathbf{F}_{\mathrm{Bernoulli}}=b\;d\;p_{\mathrm{lip}}\;\mathbf{e}_y, \quad (4)$$

where b is lip width and $\mathbf{e}_y$ is the unit vector along the y axis. A factor of $\frac{1}{2}$ in Eq. (2) implies that the displacement of the lip center is half as much as that of the tip. The symbol $\perp$ in Eq. (3) denotes the operation to derive the orthogonal vector from a vector of its operand: In the x-y coordinate system, $\mathbf{A}^{\perp}$ has the component $(-A_y, A_x)$ for any vector $\mathbf{A}=(A_x, A_y)$. Equation (3) implies that $\mathbf{F}_{\Delta p}$ has a magnitude proportional to the lip length l and a direction orthogonal to the BC side.

The origin of the x-y coordinate system is assumed to be at the center of the mouthpiece rim. As is shown in Fig. 2, the base of the lip touches the rim, so that B is on the $x=0$ plane of the mouthpiece entryway. The upper and lower lips meet on the $y=0$ plane. We denote the position of C by component as $\boldsymbol{\xi}=(\xi_x, \xi_y)$. Then, the lip opening area is given by

$$S_{\mathrm{lip}}=\max\{2b\xi_y, 0\}, \quad (5)$$

where a factor of 2 comes from the symmetric motion of the upper and lower lips.

The lip movement regulates airflow into the instrument through S_{lip}. Additionally, the lip movement directly generates flow, which is equivalent to the volume swept by the lips per unit time. This flow becomes

$$U_{\mathrm{lip}}=\left\{b(\boldsymbol{\xi}-\boldsymbol{\xi}_{\mathrm{joint}})\times\frac{d\boldsymbol{\xi}}{dt}\right\}\cdot\mathbf{e}_z$$

$$=b\left\{(\xi_x-\xi_{\mathrm{joint}_x})\,\frac{d\xi_y}{dt}-(\xi_y-\xi_{\mathrm{joint}_y})\,\frac{d\xi_x}{dt}\right\}, \quad (6)$$

where $\mathbf{e}_z$ is the unit vector parallel to the axis of swinging motion.

During closure of the lips, that is, when $S_{\mathrm{lip}}=0$, lip contact supplies another restoring force along the y axis, whose stiffness is assumed to be three times larger than k. Therefore, the supplementary restoring force $-3k\xi_y\mathbf{e}_y$ acts on the lip only when $\xi_y<0$. Similarly, lip contact yields another viscous loss of the vibrating lips, which seems large due to the lip deformation upon collision. The quality factor Q is thus assumed to decrease to less than unity on the closure condition.

By adjusting the embouchure, the brass instrument player can select notes in the harmonic series available without valve (piston) manipulation. The process of adjusting the embouchure corresponds to changing the lip eigenfrequency

TABLE I. Parameters.

Symbol	Parameter name	Value
c	speed of sound	3.4×10^2 m/s
ρ	average air density	1.2 kg/m^3
S_{cup}	area of mouthpiece entryway	2.3×10^{-4} m^2
b	width of lip opening	7.0×10^{-3} m
d	thickness of lips	2.0×10^{-3} m
$\boldsymbol{\xi}_{\text{joint}}$	lip joint position	$(0,\ 4.0)\times10^{-3}$ m
ξ_{equil_x}	x coord. of lip rest position	1.0×10^{-3} m
ξ_{equil_y}	y coord. of lip rest position	$(-0.1\text{–}2.0)\times10^{-3}$ cm
Q	lip quality factor	3.0 on the open-lip condition 0.5 on the closed-lip condition
f_{lip}	lip resonance frequency	60–700 Hz
m	lip mass	$1.5/((2\pi)^2 f_{\text{lip}})$ kg
k	Stiffness of lips	$1.5\ f_{\text{lip}}$ N/m
p_0	blowing pressure	2.0–5.0 kPa

f_{lip}. Elliott and Bowsher[5] deduced the dependence of lip mass m on the lip eigenfrequency f_{lip} from their measurements of average volume flows while various notes with different pitches were blown. Following their results, we assume that m is inversely proportional to f_{lip}. Accordingly, the behavior of stiffness k becomes proportional to f_{lip} because $f_{\text{lip}} = \sqrt{k/m}/2\pi$. Lip and other parameters for our simulations are shown in Table I.

B. Total sound production system

The sound production system comprises the lip dynamics, the airflow behavior near the lip opening, and the resonance characteristics of the instrument. These form a closed loop in the feedback system and thus self-excitation can be established. The lip dynamics has already been modeled in the previous subsection. Equations of the airflow are derived from the fluid dynamical consideration. In time domain, the acoustic response from the instrument can be calculated by a feedback equation. The same flow and feedback equations as used in the simulations with one-dimensional lip models[10] are employed in this paper and reviewed here.

Let us first review the flow equations. On the assumption of one-dimensional and incompressible flow, the mass conservation provides that the acoustical volume flow rate U_{acoust} is independent of place and depends only on time t. The region near the lip opening is divided into two parts: the upstream contraction region (i.e., the mouth cavity and the lip opening region) and the downstream expansion region (i.e., a thin region in the mouthpiece cup adjacent to the lips). In the contraction region, laminar flow is assumed to be realized, while in the expansion region, flow is assumed to come off from the boundary layer and make a jet. Therefore, we apply the energy conservation law to the flow in the former region and the momentum conservation law to the one in the latter.[14]

They become

$$p_0 - p_{\text{lip}} = \frac{1}{2}\rho\left(\frac{U_{\text{acoust}}}{S_{\text{lip}}}\right)^2 + \frac{\rho d}{S_{\text{lip}}}\frac{\partial U_{\text{acoust}}}{\partial t}, \tag{7}$$

$$p_{\text{lip}} - p = -\rho U_{\text{acoust}}^2\left(\frac{1}{S_{\text{cup}}S_{\text{lip}}} - \frac{1}{S_{\text{cup}}^2}\right), \tag{8}$$

where ρ is average air density and S_{cup} is the area of the mouthpiece entryway. The sum of Eqs. (7) and (8) implies that acoustical volume flow rate U_{acoust} is a nonlinear function of p and S_{lip}. Total volume flow rate U is given by $U = U_{\text{acoust}} + U_{\text{lip}}$, where U_{lip} is the lip-generated flow defined by Eq. (6).

The feedback equation[15] is given by the following integral equation:

$$p(t) = Z_c U(t) + \int_0^\infty ds\ r(s)\{Z_c U(t-s) + p(t-s)\}, \tag{9}$$

where $r(t)$ is the reflection function, and $Z_c = \rho c/S_{\text{cup}}$ with speed of sound c is the characteristic wave impedance of an infinite cylindrical tube having the area S_{cup}. The reflection function $r(t)$ is associated with the input impedance of the instrument $Z_{\text{in}}(f)$ through $\hat{r}(f)$ denoting the Fourier transformation of $r(t)$ as follows:

$$\hat{r}(f) = \frac{Z_{\text{in}}(f) - Z_c}{Z_{\text{in}}(f) + Z_c}. \tag{10}$$

In principle, the reflection function $r(t)$ is causal. This is guaranteed by the nature of the input impedance $Z_{\text{in}}(f)$ representing causal acoustic responses from the instrument. However, there may be cases in which the numerical calculation from $Z_{\text{in}}(f)$ by way of Eq. (10) may affect the causality of $r(t)$: The wake of nonzero $r(t)$ for $t>0$ penetrates into the $t<0$ region. This is due to a finite cutoff frequency or sampling frequency associated with the numerical calculation. In this case, $r(t)$ cannot be used in Eq. (9) as it stands. For the brass instrument, abrupt reflections from the mouthpiece generally cause this difficulty. To avoid this, we employ a causal reflection function $r^c(t)$, which was used in the previous simulation with one-dimensional lip models.[10] In brief, $r^c(t)$ is defined by two times the even component (with respect to the time reversal $t \leftrightarrow -t$) of the original $r(t)$ for $t \geqslant 0$ and zero for $t<0$. To verify this procedure, it has been confirmed that Eq. (9) with the causal reflection function $r^c(t)$ simulates a ratio of generated pressure p to input flow U, reproducing almost the same input impedance.

The data of $Z_{\text{in}}(f)$ used in this paper are the same ones used in the previous simulation which were calculated from the dimensions of a real B$^\flat$ trumpet with some assumptions on the acoustics. The magnitude and phase of $Z_{\text{in}}(f)$ are shown in Fig. 3. Table II lists the magnitudes (normalized by Z_c), frequencies of the impedance peaks, and their frequency intervals. The impedance peaks, which are at nearly equal intervals with the exception of the first peak, correspond to the resonance modes of the instrument. The envelope of these peaks is characteristic of the brass instrument. Note that the sign of the phase $\angle Z_{\text{in}}(f)$ changes from positive to negative as frequency f rises and sweeps resonance frequencies. These characteristics of this $Z_{\text{in}}(f)$ are very similar to the input impedances obtained in experiments.[16–18] Therefore, the general acoustical behavior of the real brass instrument is expected to be reproduced by the total simulation system.

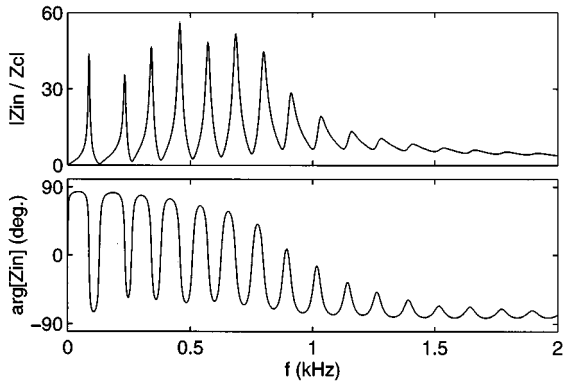

FIG. 3. The magnitude and phase angle of input impedance Z_{in} scaled by the characteristic wave impedance Z_c, which is calculated from the shape of an actual $B^{\flat}$ trumpet.

II. SIMULATION

The oscillation is described by the variables of lip position $\boldsymbol{\xi}(t)$, mouthpiece pressure $p(t)$, lip opening pressure $p_{\mathrm{lip}}(t)$, acoustic volume velocity $U_{\mathrm{acoust}}(t)$, lip-generated volume velocity $U_{\mathrm{lip}}(t)$, and lip opening area $S_{\mathrm{lip}}(t)$. These variables satisfy the equations developed in the previous section. A time-domain simulation is carried out algorithmically as follows:

(1) Suppose the variables $\boldsymbol{\xi}$, p, p_{lip}, U_{acoust}, U_{lip}, and S_{lip} are all known at all times earlier than the present, solve the equation of the lip motion (1), and find the new $\boldsymbol{\xi}$ at the time one step ahead.
(2) Calculate the new S_{lip} and U_{lip} defined by Eqs. (5) and (6), respectively.
(3) With the new S_{lip}, U_{lip}, and past data of p and $U=U_{\mathrm{acoust}}+U_{\mathrm{lip}}$, solve the flow equation [i.e., sum of Eqs. (7) and (8)] and the feedback equation (9) simultaneously, and obtain the new p and U_{acoust}.
(4) Solve Eq. (8) to obtain the new p_{lip}.
(5) Update time by one step, and then return to (1).

The parameters of lip geometry, $\boldsymbol{\xi}_{\mathrm{joint}}$, $\boldsymbol{\xi}_{\mathrm{equil}}$, b, and d, and the blowing pressure p_0 are fixed during one attempt of the simulation. The initial values of p, p_{lip}, U_{acoust}, and U_{lip} are all zeros. The lip position $\boldsymbol{\xi}$ is initially placed at the rest position $\boldsymbol{\xi}_{\mathrm{equil}}$. The forward Euler method to discretize the differential equations and the trapezoidal approximation for the integration are used with 8-kHz sampling frequency.

TABLE II. Magnitudes and frequencies of input impedance peaks and their intervals.

Mode		$\lvert Z_{in}/Z_c\rvert$	f_{peak} (Hz)	Δf (Hz)
I	Pd	43.7	87	
II	$B_3^{\flat}$	35.2	232	145
III	F_4	46.4	341	109
IV	$B_4^{\flat}$	55.7	457	116
V	D_5	48.1	572	115
VI	F_5	51.6	686	114
VII	$A_5^{\flat}$	44.5	800	114
VIII	$B_5^{\flat}$	28.5	913	113

Despite the simple method and the low sampling frequency, we did not encounter apparent numerical instabilities. This partly assures the validity of the simulation method. For greater validity, some of the oscillations were additionally calculated with 48-kHz sampling frequency. They had almost the same waveforms as the ones calculated with the original 8-kHz sampling frequency. In particular, the phase relations among $p(t)$, $U(t)$, and $S_{\mathrm{lip}}(t)$, which will be investigated later, did not change with this oversampling.

A. Mode selection

By changing lip eigenfrequency f_{lip} from 60 through 700 Hz at intervals of 20 Hz (except 600, 620, and 700 Hz, at which no stable self-excitation is generated), we obtained stable self-excited trumpet sounds for the first through sixth resonance modes. Blowing pressure p_0 for the moderate (mf) sound level was set at 2.0, 2.5, 3.0, 3.5, 4.0, and 5.0 kPa for the first through sixth modes, respectively. These values were chosen so as to match the measurements of mouth pressures for various notes blown on brass instruments,[19] although the great variety among the trials and players was reported.

The y component of the lip equilibrium position ξ_{equil_y}, which determines the average lip opening area, was adjusted so that the following criteria were satisfied: (1) The lips do not come into contact with each other or only have contact in a much shorter time than the oscillation period and (2) the maximum amplitude of oscillation is obtained. With these criteria, ξ_{equil_y} can be practically determined as a function of f_{lip} and p_0 and therefore ceases to be an independent parameter.

The other parameters of lip geometry, b, d, $\boldsymbol{\xi}_{\mathrm{joint}}$, and ξ_{equil_x}, were all fixed at the values listed in Table I. Due to the simplified model, these parameters are not directly related to the actual dimensions of the player's lips. However, they were selected to be consistent with the dimensions of the lips put to a trumpet mouthpiece.

Figure 4 plots the frequency of self-excited sound f_{sound} against the lip eigenfrequency f_{lip} with the first through sixth resonance frequencies of the trumpet depicted with dash-dot lines. The first through sixth resonance modes appear. Between adjacent resonance modes, frequency gaps that represent the mode transition are found. In each resonance mode, sounding frequency f_{sound} does not take a constant value. Instead, there is a frequency range of f_{sound}, where self-excitation is possible and where f_{sound} gradually ascends with increases in f_{lip}. It is noteworthy that in the first, second and third modes the possible ranges of f_{sound} span both the higher and lower sides of the resonance frequencies, whereas in the fourth, fifth, and sixth modes, they are only on the lower sides.

Within each resonance mode, especially in the third and fourth, the slope of the sounding frequency is less steep at the higher frequency range than at the lower frequency range. In other words, the sounding frequency is insensitive for any perturbation of f_{lip} at the higher frequency range. From the player's point of view, blowing a note at as high a frequency as possible is preferable, because the insensitivity brings the ease of maintaining a given playing frequency. As

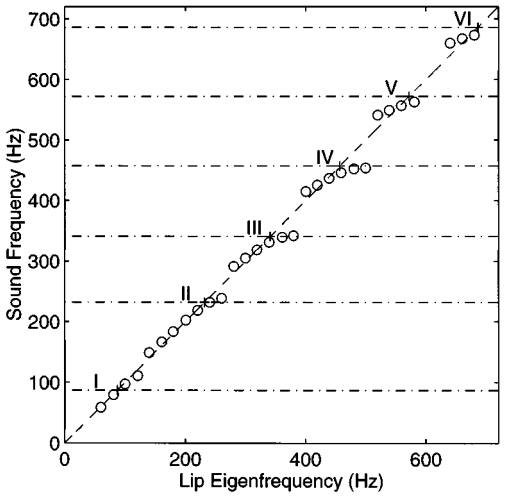

FIG. 4. Frequency (depicted with ○) of self-excited sound against the lip eigenfrequency. The dash-dot lines represent the first through sixth resonance frequencies of the instrument. In the first through third modes, self-excitation occurs with sounding frequencies both higher and lower than the resonance frequencies, whereas in the fourth and higher modes, it only occurs with a sounding frequency lower than the resonance frequencies.

a result, the actual blowing in the lower modes such as the second and third would be executed on the higher frequency side of the impedance peaks. However, in the higher modes, it would still be executed on the lower side, because the possible frequency ranges are lower than the resonance frequencies.

B. Oscillating quantities

Apart from selecting resonance modes by adjusting the embouchure, the brass instrument player finely controls the embouchure to make a blown note have both stable frequency and sufficient amplitude. Such notes selected from the different modes should also be relatively in tune. To mimic the player's embouchure control in the simulation system, we change the lip eigenfrequency f_{lip} at intervals of 10 Hz, instead of the 20 Hz used in the previous subsection, and find the optimum oscillation of each mode by the following procedure: First, search for the maximum f_{lip} that provides oscillation with the highest frequency; then, lower the f_{lip} 10 Hz to obtain an oscillation with both stable frequency and sufficient amplitude.

Waveforms and the lip trajectories of these oscillations in the second through sixth modes are depicted in Fig. 5(a)–(e). A ''loose-lipping'' tone[20] [Fig. 5(f)], which is an oscillation an octave below the normal oscillation in the third mode, is also compared with the normal oscillations in Fig. 5. It is found that the characteristic waveform with rich harmonics turns out to be a sinusoidal one from the lower to the higher modes, which is very similar to the change in the observed brass sound.[5,21] The sinusoidal waveforms of S_{lip} in all resonance modes whose amplitude decreases as the mode rises reproduce the result of Martin's observation of lip movement.[2]

The counterclockwise trajectory of the lip displacement $\boldsymbol{\xi}$, whose amplitude is decreased as the mode rises, is again in accord with Martin's observation. There is also a tendency for the long axis of the oval trajectory to gradually tilt from the direction parallel to the airflow in the second mode (a) toward a certain angle in the higher modes (b)–(e). This qualitatively corresponds to the change in lip vibration state from swinging motion dominant to stretching motion dominant.

For a loose-lipping tone, it is found that the amplitude of the lip motion and volume flow rate U are much larger than those of the normal oscillations, although the pressure amplitude is almost the same. The tilted direction of the trajectory in (f) implies the stretching motion dominant lip vibration state.

The trajectory for the loose-lipping tone can be compared with the two-dimensional motion of a trombone player's upper lip measured by Copley and Strong,[4] because the frequency of 166 Hz is close to that of their measured F_3 tones. The amplitude and flatness of the simulated trajectory are in broad agreement with those of the measured trajectory. However, the measured trajectory has the long axis roughly along the y axis, while our simulated trajectory has the one roughly along the x axis. This is probably because of the larger dimensions of the trombone mouthpiece cup, which allows the lips to get into the cup more deeply.

The phase differences $\angle p-\angle U$ and $\angle S_{\mathrm{lip}}-\angle p$ in the oscillations shown in Fig. 5 are listed along with resonance frequencies of the instrument (frequencies of the impedance peak) f_{peak}, lip eigenfrequencies f_{lip}, and sounding frequencies f_{sound} in Table III. It is found that $\angle p-\angle U$ changes from negative values in the second and third modes to positive values in the fourth and higher modes. This corresponds to the change in the sides of the impedance peaks on which the oscillation occurs in different modes, which is manifest in comparing f_{peak} with f_{sound}. The phase difference $\angle S_{\mathrm{lip}}-\angle p$ is positive in the first through fourth modes and negative in the fifth and sixth modes. This change proves that the lip motion changes from the swinging motion dominant state in the first through fourth modes to the stretching motion dominant state in the fifth and sixth modes.

The condition derived by the linear theory of oscillation that these two phase differences $\angle p-\angle U$ and $\angle S_{\mathrm{lip}}-\angle p$ have the same absolute values and have opposite signs is not always satisfied. Especially in the fourth mode, the signs of these phase differences are both positive and the stretching motion dominant state inferred from positive $\angle p-\angle U$ contradicts the swinging motion dominant state that is actually excited.

III. DISCUSSION

The results of the simulation with the two-dimensional lip vibration models are significantly different from those with the one-dimensional models in the following points:

(1) The sounding frequency f_{sound} is not far from the lip eigenfrequency f_{lip}.
(2) A transition in lip vibration states is observed. The swinging motion dominant oscillation typical in the lower resonance modes gives way to the stretching motion dominant oscillation in the higher modes.

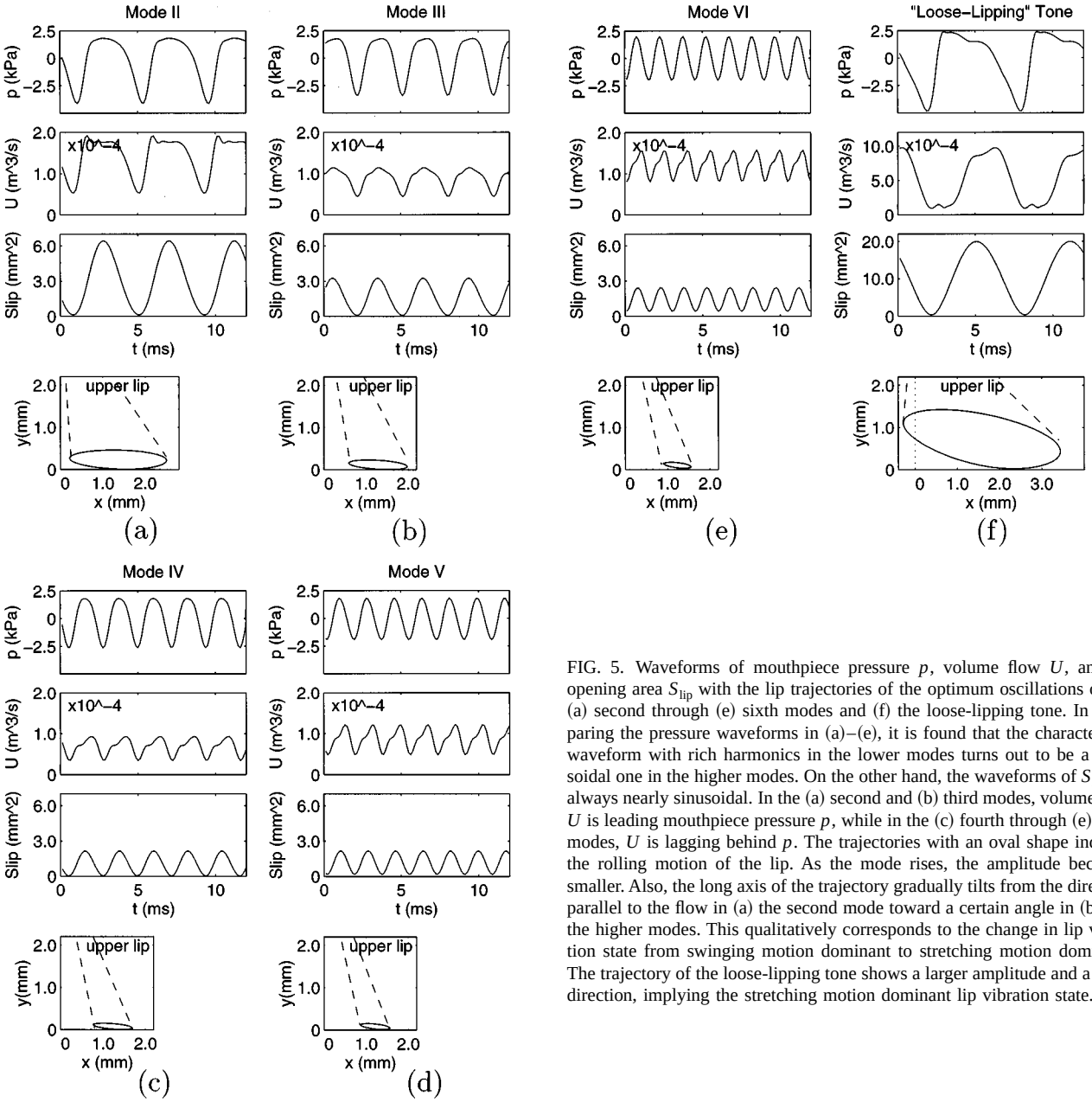

FIG. 5. Waveforms of mouthpiece pressure p, volume flow U, and lip opening area S_{lip} with the lip trajectories of the optimum oscillations of the (a) second through (e) sixth modes and (f) the loose-lipping tone. In comparing the pressure waveforms in (a)–(e), it is found that the characteristic waveform with rich harmonics in the lower modes turns out to be a sinusoidal one in the higher modes. On the other hand, the waveforms of S_{lip} are always nearly sinusoidal. In the (a) second and (b) third modes, volume flow U is leading mouthpiece pressure p, while in the (c) fourth through (e) sixth modes, U is lagging behind p. The trajectories with an oval shape indicate the rolling motion of the lip. As the mode rises, the amplitude becomes smaller. Also, the long axis of the trajectory gradually tilts from the direction parallel to the flow in (a) the second mode toward a certain angle in (b)–(e) the higher modes. This qualitatively corresponds to the change in lip vibration state from swinging motion dominant to stretching motion dominant. The trajectory of the loose-lipping tone shows a larger amplitude and a tilted direction, implying the stretching motion dominant lip vibration state.

Let us discuss the causes of these characteristics within the scope of the linear theory of oscillation, where the flow equations (7) and (8) are linearized and lip collision is omitted. For simplicity, we assume $S_{\mathrm{lip}} \ll S_{\mathrm{cup}}$ and thus $p_{\mathrm{lip}}=p$, which implies no pressure recovery at the mouthpiece cup, holds. As $U_{\mathrm{lip}} \ll U_{\mathrm{acoust}}$ is approximately satisfied in the simulation, the effect of U_{lip} is excluded from this discussion.

To make the discussion precise, we define

$$G(f)=\frac{S_{\mathrm{lip}}(f)}{p(f)}, \tag{11}$$

where $S_{\mathrm{lip}}(f)$ and $p(f)$ denote Fourier components of S_{lip} and p, respectively. As $G(f)$ represents a response of the lip motion to the driving pressure, we here call $G(f)$ the lip mobility, although $G(f)$ is only one component of the lip mobility having a tensor form. It is only this component $G(f)$ that plays a crucial role in considering the oscillation conditions of the total sound production system. Generally, the magnitude of $G(f)$ has a peak near the lip eigenfrequency f_{lip}, whereas the frequency dependence of phase $\angle G(f)=\angle S_{\mathrm{lip}}(f)-\angle p(f)$ is specific to the lip vibration model.

The regeneration theory,[5,9] regardless of what lip dynamics is assumed, requires oscillation to have sounding frequency f satisfying the following magnitude and phase conditions:

$$\sqrt{\frac{2p_0}{\rho}}\,|G(f)||Z_{\mathrm{in}}(f)| \geq 1, \tag{12}$$

$$\angle G(f)+\angle Z_{\mathrm{in}}(f)=0. \tag{13}$$

The magnitude condition indicates that oscillation is more likely to be generated with larger blowing pressure and stronger resonances of the instrument and the lip. We have

TABLE III. Lip eigenfrequencies, sound frequencies, phase differences $\angle p - \angle U$ and $\angle S_{\rm lip} - \angle p$ of the optimum oscillation of each resonance mode and the loose-lipping tone.

Oscillation	Note	$f_{\rm peak}$ (Hz)	$f_{\rm lip}$ (Hz)	$f_{\rm sound}$ (Hz)	$\angle p - \angle U$ (deg)	$\angle S_{\rm lip} - \angle p$ (deg)
II	$B_3^\flat$	232	250	236	−25.6	18.1
III	F_4	341	370	342	−3.2	12.5
IV	$B_4^\flat$	457	490	453	27.7	5.4
V	D_5	572	580	563	41.9	−7.0
VI	F_5	686	680	673	38.5	−7.6
Loose-lipping	(F_3)	232	160	166	81.6	−41.5

already investigated the phase condition in the Introduction and Sec. II B, although $G(f)$ was not defined there.

Before calculating the lip mobility $G(f)$ for the two-dimensional lip vibration model, let us first obtain the time-averaged or dc component of the lip displacement $\boldsymbol{\xi}^{\rm dc} = (\xi_x^{\rm dc},\ \xi_y^{\rm dc})$. The equation of lip motion (1), or, in this case, the balance equation of forces acting on the lip becomes

$$\begin{pmatrix} \frac{k}{2} & bp_0 \\ -bp_0 & \frac{k}{2} \end{pmatrix} \begin{pmatrix} \xi_x^{\rm dc} \\ \xi_y^{\rm dc} \end{pmatrix} = \begin{pmatrix} \frac{k}{2}\,\xi_{{\rm equil}_x} + bp_0\xi_{{\rm joint}_y} \\ \frac{k}{2}\,\xi_{{\rm equil}_y} \end{pmatrix}, \tag{14}$$

because the time-averaged mouthpiece pressure $p^{\rm dc}$ is zero. Equation (14) can be solved as

$$\begin{pmatrix} \xi_x^{\rm dc} \\ \xi_y^{\rm dc} \end{pmatrix} = \frac{1}{\left(\frac{k}{2}\right)^2 + (bp_0)^2} \times \begin{pmatrix} \left(\frac{k}{2}\right)^2 \xi_{{\rm equil}_x} + \frac{k}{2}\,bp_0(\xi_{{\rm joint}_y} - \xi_{{\rm equil}_y}) \\ \left(\frac{k}{2}\right)^2 \xi_{{\rm equil}_y} + \frac{k}{2}\,bp_0\xi_{{\rm equil}_x} + (bp_0)^2\xi_{{\rm joint}_y} \end{pmatrix}. \tag{15}$$

We express the time-varying or ac component of the lip displacement with $\boldsymbol{\xi}^{\rm ac} = (\xi_x^{\rm ac},\ \xi_y^{\rm ac})$. The equation of lip motion (1) gives a linear equation for $\boldsymbol{\xi}^{\rm ac}$ in the frequency domain as follows:

$$\begin{pmatrix} \frac{k}{2}\,\Lambda^{-1}(f/f_{\rm lip}) & bp_0 \\ -bp_0 & \frac{k}{2}\,\Lambda^{-1}(f/f_{\rm lip}) \end{pmatrix} \begin{pmatrix} \xi_x^{\rm ac} \\ \xi_y^{\rm ac} \end{pmatrix} = \begin{pmatrix} -b\xi_{{\rm joint}_y} \\ -b\xi_x^{\rm dc} + bd \end{pmatrix} p, \tag{16}$$

where the quadratic term $\xi_y^{\rm ac} p$ is omitted, because the amplitude of lip motion is sufficiently smaller than the lip length. The function $\Lambda(\Omega)$ in Eq. (16) is defined by

$$\Lambda(\Omega) = \frac{1}{1 - \Omega^2 + i(\Omega/Q)}. \tag{17}$$

From the solution of Eq. (16), the lip mobility $G(f)$ is calculated as

$$G(f) = \frac{2b\xi_y^{\rm ac}(f)}{p(f)} = (2b)^2\,\frac{(d - \xi_x^{\rm dc}) - 2b\xi_{{\rm joint}_y}\,p_0\{\Lambda(f/f_{\rm lip})/k\}}{1 + [2bp_0\{\Lambda(f/f_{\rm lip})/k\}]^2}\,\frac{\Lambda(f/f_{\rm lip})}{k}. \tag{18}$$

The calculation results of the magnitude and phase of $G(f)$ for $f_{\rm lip}$=250 Hz and $f_{\rm lip}$=580 Hz are depicted in Fig. 6(a) and (b), respectively. For comparison, those of lip mobility in the one-dimensional transverse model are also drawn with broken lines. Near the lip eigenfrequency $f_{\rm lip}$, the phase of $G(f)$ takes a value around −30° in (a) and one around −45° in (b). Because the phase of $Z_{\rm in}$ changes suddenly from a value less than 90° to another larger than −90°C near the resonance frequencies, frequency f satisfying the phase condition (13) is likely to exist near the lip eigenfrequency $f_{\rm lip}$. For the transverse model (broken lines), $\angle G(f)$ is around −90° near $f_{\rm lip}$ in both (a) and (b). This implies that frequency f should be considerably off to the lower side of $f_{\rm lip}$ so that the phase becomes closer to zero and the phase condition is satisfied. Therefore, the characteristics of $\angle G$ near the lip eigenfrequency in the two-dimensional model successfully explain why the sounding

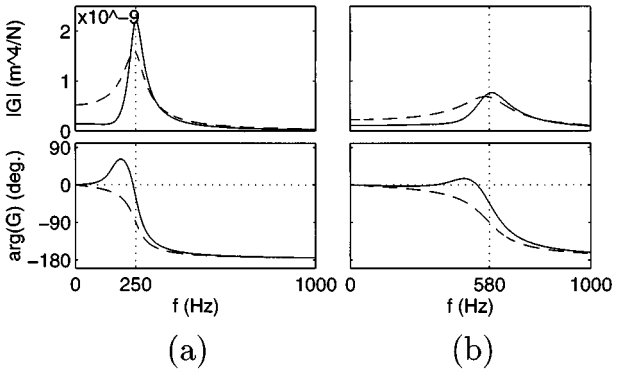

FIG. 6. Calculation results of the magnitude and phase of the lip mobility $G(f)$ for lip eigenfrequency $f_{\rm lip}$=250 Hz (a) and 580 Hz (b). The solid lines denote results for the two-dimensional lip vibration model, and the broken lines denote those for the one-dimensional transverse model. The peak of the magnitude indicates the resonance of lip vibration. A frequency region having a positive phase of $G(f)$ is found in the two-dimensional model. In this region, the swinging motion of lip vibration is dominant, whereas in the $\angle G$-negative region the stretching motion becomes dominant. Note that the $\angle G$-positive region is very close to $f_{\rm lip}$ in (a), while it is far from $f_{\rm lip}$ in (b). This difference causes the transition of the lip vibration state.

frequency f_{sound} is not far from the lip eigenfrequency f_{lip}.

Let us now compare (a) with (b) in Fig. 6. In these phase plots, we find the frequency region having a positive phase of $G(f)$ (the $\angle G$-positive region), where the swinging motion is dominant. Note that in (a) the $\angle G$-positive region is very close to the lip eigenfrequency f_{lip} where the magnitude of $G(f)$ takes the maximum. On the other hand, in (b) the $\angle G$-positive region is far from f_{lip}. Therefore, for the lower modes like the second shown in (a), there exists f that gives sufficiently large $|G(f)|$ so as to satisfy the magnitude condition (12) both in the $\angle G$-positive and negative regions. In actual blowing, such f in the $\angle G$-positive region is chosen for the frequency stability of a played note. However, for the higher modes such as the fifth in (b), f satisfying the magnitude condition (12) is not found in the $\angle G$-positive region but only in the $\angle G$-negative region, where the stretching motion is dominant. This explains why the lip vibration state changes from swinging motion dominant in the lower modes to stretching motion dominant in the higher modes.

The investigation of the oscillation conditions (12) and (13) shows the advantage of the two-dimensional lip vibration model over the one-dimensional models as the generator of the brass instrument. The magnitude condition (12) allows the system to oscillate only in the presence of large resonances of both the instrument and the lip. The input impedance $Z_{\text{in}}(f)$ has a maximum magnitude at one of the resonance frequencies and the lip mobility $G(f)$ is maximized at the lip eigenfrequency. Therefore, the system will obtain the optimal effect of these resonances when the oscillation frequency f is close to the lip eigenfrequency and to one of the air-column resonance frequencies. On the other hand, the phase condition (13) constrains the phases of $Z_{\text{in}}(f)$ and $G(f)$ to cancel each other. At one of the air-column resonance frequencies, where the maximum resonance of the instrument is obtained, $\angle Z_{\text{in}}(f)$ is approximately zero. To satisfy the phase condition, $\angle G(f)$ should also be as close to zero as possible. In the two-dimensional model, this is compatible with the magnitude condition because $\angle G(f)$ vanishes near the lip eigenfrequency that maximizes the magnitude of $G(f)$. In the one-dimensional lip vibration models, however, this conflicts with the magnitude condition because $\angle G(f)$ is around $\pm 90°$ near the lip eigenfrequency.

To understand the mechanism of change in lip vibration states further, let us go back to the lip mobility $G(f)$ calculated in Eq. (18). The first term in the numerator of the second factor in Eq. (18) corresponds to the effect of the stretching motion of the lip directly driven by the Bernoulli pressure along the y direction. The second term in the same numerator represents the effect of the lip movement along the y direction, which is caused by that along the x direction (i.e., the swinging motion of $\boldsymbol{\xi}^{\text{ac}}$). Note that the second term is inversely proportional to the lip stiffness k, which controls the amplitude of the lip motion. This is related to the swinging motion of $\boldsymbol{\xi}^{\text{ac}}$ being generated by torque that is the product of the force acting on the lip and the amplitude of the motion. In the lower resonance modes, these two terms are comparable and the second term surpasses the first one when the sounding frequency is near the lip eigenfrequency due to a large magnitude of Λ representing the lip resonance. As the mode rises, the amplitude of oscillation becomes smaller due to the lip stiffness k that is adjusted to increase proportionally to the lip eigenfrequency f_{lip}. This causes a decline in the swinging motion due to the decrease in the second term. In the higher modes, therefore, the first term is always dominant and only the stretching motion dominant state is realized.

The parameters of lip shape certainly alter the character of the lip mobility $G(f)$. In particular, the ratio of lip thickness to lip length, which is approximately equal to d/ξ_{joint_y}, affects the frequency region having a positive phase of $G(f)$. This indicates that this ratio can control the critical resonance mode at which the lip vibration state changes from swinging motion dominant to stretching motion dominant. Nevertheless, the mechanism that yields the transition between the lip vibration states would be retained, regardless of the selection of lip shape parameters, in the two-dimensional lip vibration model investigated in this paper. In actual blowing, the ratio d/ξ_{joint_y} may be controlled by the embouchure. If this is the case, an increase in the ratio d/ξ_{joint_y} would enhance the transition; however, this effect was not investigated in this simulation.

IV. CONCLUSIONS

By adopting the two-dimensional lip vibration model, where the lips execute both swinging and stretching motions, the whole system successfully simulates self-excited trumpet sounds in the first through sixth resonance modes. In the first through third modes, oscillations occur on both the lower and higher frequency sides of the resonance frequency of the instrument, while in the fourth and higher modes they are realized only on the lower sides. In each resonance mode, the oscillation having the highest frequency and sufficient amplitude, which appears to be actually blown, is selected as the optimum oscillation of the mode. The phase differences between the lip vibration and the mouthpiece pressure of these oscillations in the first through fourth modes are positive and those in the fifth and sixth modes are negative.

The phase relations obtained here can be compared with those of the one-dimensional lip models. In the lower modes the two-dimensional lip model operates in the same way as the one-dimensional swinging-door model, while in the higher modes this model operates in the same way as the one-dimensional transverse model. Accordingly, it can be concluded that the two-dimensional lip model closely replicates the transition of the lip vibration states observed in Yoshikawa's experiment.

The change from the positive phase difference in the lower modes to the negative one in the higher modes results from the dynamics of the lip model itself. In the lower modes, the large amplitude of lip motion enhances the swinging motion, whereas in the higher modes the small amplitude suppresses the swinging motion and the stretching motion becomes dominant. The mechanism that yields the transition of the phase relation is not limited to this two-dimensional model. Rather, it will be incorporated into future models with many degrees of freedom, provided that the

modeled lip is capable of both swinging outward and stretching along the lip length.

In actual lip vibration, there may be other possible causes for the transition, such as lip deformation in embouchure change. However, the lip dynamics of this two-dimensional lip vibration model provide one of the most plausible explanations for the transition of the lip vibration states.

ACKNOWLEDGMENTS

The authors wish to thank Hiroyuki Ohtsuki and Hiroshi Tamagawa for useful discussions and their programming assistance. One of the authors (S.A.) wishes to thank Professor William J. Strong for his careful reviews of the manuscript, and Dr. Shigeru Yoshikawa for his valuable comments and continuing encouragement.

[1] H. L. F. Helmholtz, *On the Sensations of Tone* (Dover, New York, reprinted 1954).
[2] D. W. Martin, ''Lip vibrations in a cornet mouthpiece,'' J. Acoust. Soc. Am. **13**, 305–308 (1942).
[3] H. L. Leno, in D. E. Hall, *Musical Acoustics* (Brooks/Cole, Pacific Grove, 1991), 2nd ed., p. 264.
[4] D. C. Copley and W. J. Strong, ''A stroboscopic study of lip vibrations in a trombone,'' J. Acoust. Soc. Am. **99**, 1219–1226 (1996).
[5] S. J. Elliott and J. M. Bowsher, ''Regeneration in brass wind instruments,'' J. Sound Vib. **83**(2), 181–217 (1982).
[6] J. Saneyoshi, H. Teramura, and S. Yoshikawa, ''Feedback oscillations in reed woodwind and brasswind instruments,'' Acustica **62**, 194–210 (1987).
[7] They mistakenly referred to this model as a model of the inward-striking reed in their paper, but this terminology is incorrect.
[8] N. H. Fletcher, ''Autonomous vibration of simple pressure-controlled valves in gas flows,'' J. Acoust. Soc. Am. **93**, 2172–2180 (1993).
[9] N. H. Fletcher, ''Excitation mechanisms in woodwind and brass instruments,'' Acustica **43**, 63–72 (1979).
[10] S. Adachi and M. Sato, ''Time-domain simulation of sound production in the brass instrument,'' J. Acoust. Soc. Am. **97**, 3850–3861 (1995).
[11] D. H. Keefe, ''On sound production in brass instruments,'' J. Acoust. Soc. Am. **87**, S138 (1990).
[12] W. J. Strong and J. D. Dudley, ''Simulation of a player-trumpet system,'' in Proceedings of the Stockholm Musical Acoustics Conference, 1993, pp. 520–524.
[13] S. Yoshikawa, ''Acoustical behavior of brass player's lips,'' J. Acoust. Soc. Am. **97**, 1929–1939 (1995).
[14] K. Ishizaka and J. L. Flanagan, ''Synthesis of voiced sounds from a two-mass model of the vocal cords,'' Bell Syst. Tech. J. **51**, 1233–1268 (1972).
[15] R. T. Schumacher, ''*Ab initio* calculations of the oscillations of a clarinet,'' Acustica **48**, 71–85 (1981).
[16] A. H. Benade, ''The physics of brasses,'' Sci. Am. **299**, 24–35 (July 1973).
[17] J. Backus, ''Input impedance curves for the brass instruments,'' J. Acoust. Soc. Am. **60**, 470–480 (1976).
[18] R. Caussé, J. Kergomard, and X. Lurton, ''Input impedance of brass musical instruments—Comparison between experiments and numerical models,'' J. Acoust. Soc. Am. **75**, 241–254 (1984).
[19] Results of the measurements by several authors are summarized in Ref. 5.
[20] A. Baines, *Brass Instruments: Their History and Development* (Faber and Faber, London, 1976).
[21] J. Backus and T. C. Hundley, ''Harmonic generation in the trumpet,'' J. Acoust. Soc. Am. **49**, 509–519 (1971).